



In the format provided by the authors and unedited.

Fine tuning the extracellular environment accelerates the derivation of kidney organoids from human pluripotent stem cells

Elena Garreta^{1,11}, Patricia Prado^{1,11}, Carolina Tarantino¹, Roger Oria ^{2,3}, Lucia Fanlo⁴, Elisa Martí⁴, Dobryna Zalvidea², Xavier Trepát^{2,3,5,6}, Pere Roca-Cusachs^{2,3}, Aleix Gavaldà-Navarro⁷, Luca Cozzuto⁸, Josep M. Campistol⁹, Juan Carlos Izpisúa Belmonte¹⁰, Carmen Hurtado del Pozo¹ and Nuria Montserrat ^{1,5,6*}

¹Pluripotency for Organ Regeneration, Institute for Bioengineering of Catalonia (IBEC), The Barcelona Institute of Technology (BIST), Barcelona, Spain.

²Institute for Bioengineering of Catalonia (IBEC), The Barcelona Institute of Technology (BIST), Barcelona, Spain. ³University of Barcelona, Barcelona, Spain.

⁴Instituto de Biología Molecular de Barcelona (IBMB-CSIC), Parc Científic de Barcelona, Barcelona, Spain. ⁵Centro de Investigación Biomédica en Red en Bioingeniería, Biomateriales y Nanomedicina, Madrid, Spain.

⁶Catalan Institution for Research and Advanced Studies (ICREA), Barcelona, Spain.

⁷Departament de Bioquímica i Biomedicina Molecular, Institut de Biomedicina (IBUB), Universitat de Barcelona and CIBER Fisiopatología de la Obesidad y Nutrición, Barcelona, Spain.

⁸Centre for Genomic Regulation (CRG), The Barcelona Institute of Science and Technology, Barcelona, Spain. ⁹Hospital Clinic, University of Barcelona, IDIBAPS, Barcelona, Spain.

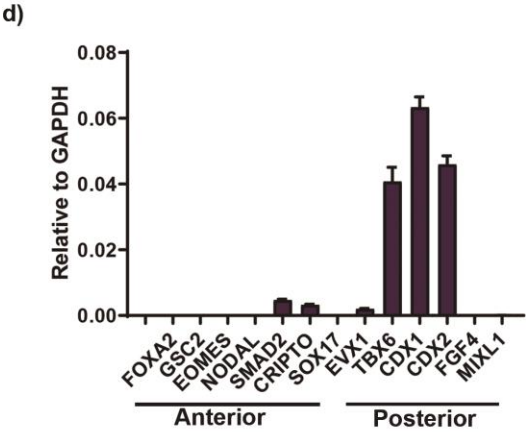
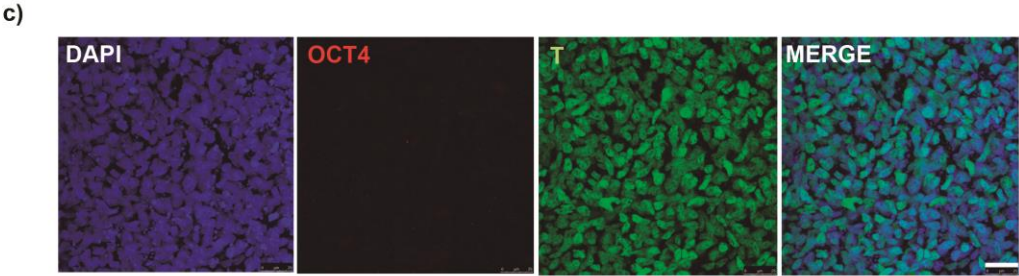
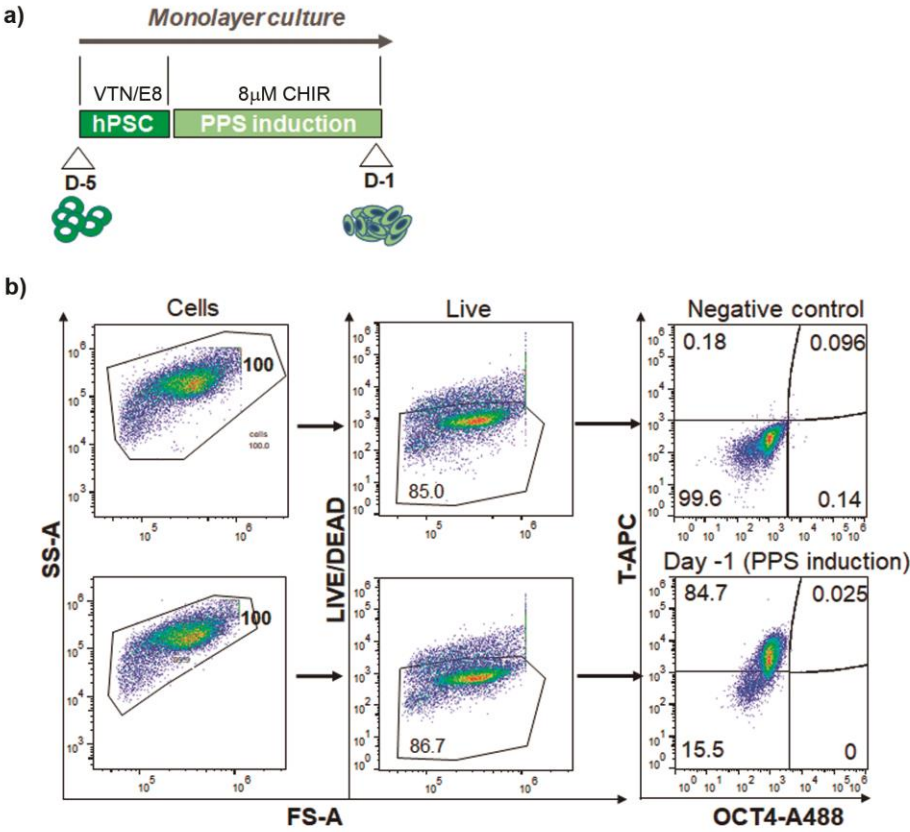
¹⁰Gene Expression Laboratory, Salk Institute for Biological Studies, La Jolla, CA, USA. ¹¹These authors contributed equally: Elena Garreta, Patricia Prado. *e-mail: nmontserrat@ibecbarcelona.eu

Supplementary information

This document contains:

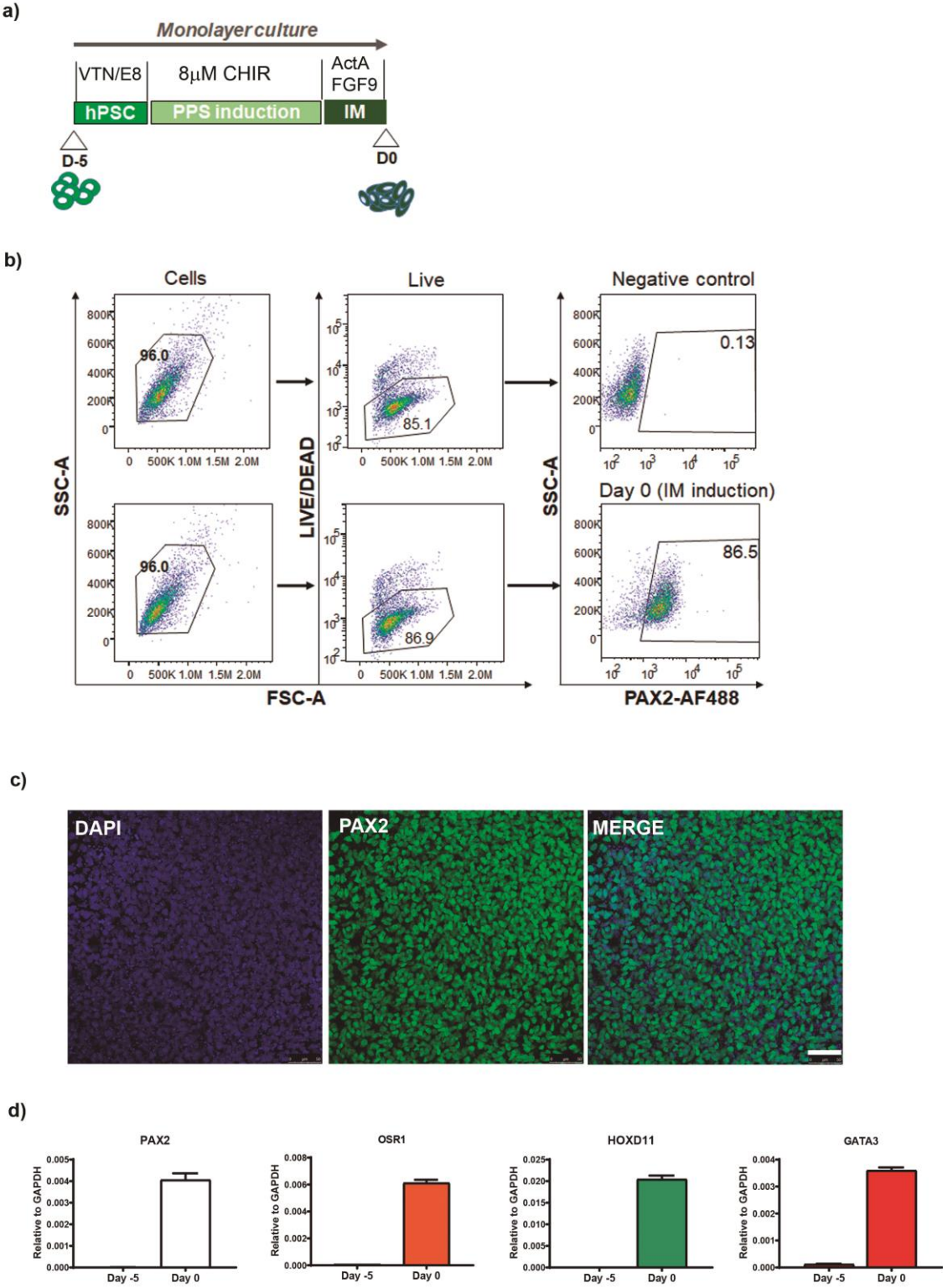
- Supplementary Figures 1 to 17
- Legends for Supplementary Tables 1 to 5, and supplementary Table 7 (provided as separate excel files)
- Supplementary Table 6
- Legends for Supplementary Videos 1 to 3

Supplementary Figure 1



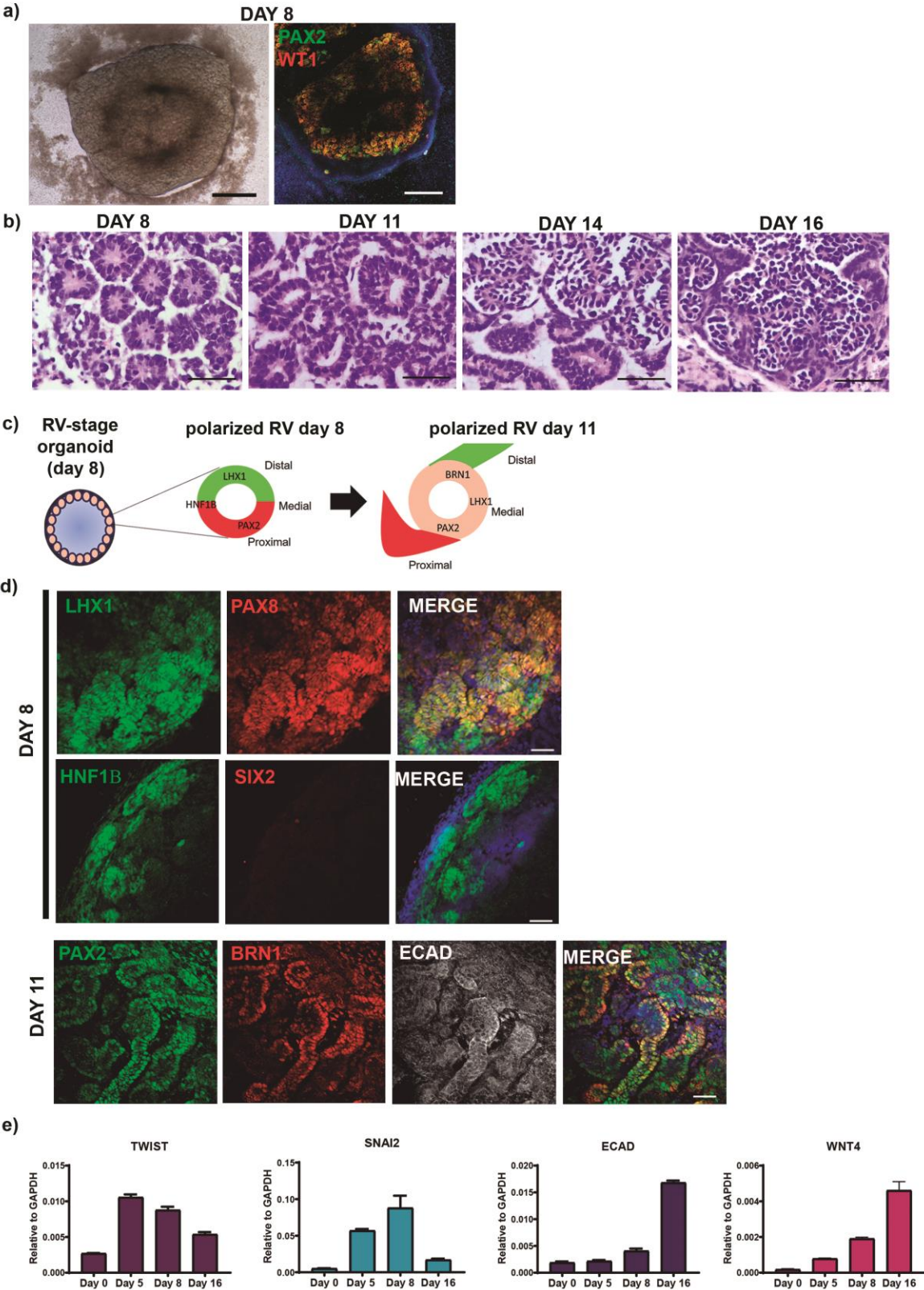
Supplementary Fig. 1 | Induction of PPS-committed cells from hPSC. **a**, Schematic of the timeline for the directed differentiation of hPSCs (*day -5*) into PPS-committed cells by 3-day exposure to 8 μ M CHIR in 2D monolayer culture (*day -1*). **b**, Flow cytometry analysis for the intracellular staining of brachyury (referred as T) and OCT4 in PPS-committed cells (*day -1*). Numbers in quadrants indicate percent cells in each. Data are representative of three independent experiments. The mean percentage of T⁺ OCT4⁻ cells is 82.2 ± 2.6 % (mean \pm SD, n = 3). **c**, Immunocytochemistry for T and OCT4 expression after PPS induction (*day -1*). Scale bars, 25 μ m. Images are representative of four independent experiments. **d**, qPCR analysis for APS and PPS markers after PPS induction (*day -1*). Genes are indicated. Data are mean \pm SD (technical replicates). The experiment was repeated independently two times with similar results.

Supplementary Figure 2



Supplementary Fig. 2 | Differentiation of hPSC-derived PPS cells into IM cells. **a**, Schematic of the timeline for the directed differentiation of hPSCs (*day -5*) into IM-committed cells (*day 0*). After PPS induction (*day -1*), treatment with FGF9 and Activin A for 1 day promotes the efficient generation of IM-committed cells (*day 0*). **b**, Flow cytometry analysis for the intracellular staining of PAX2 in IM-committed cells (*day 0*). Numbers in outlined areas indicate percent cells. Data are representative of three independent experiments. The mean percentage of PAX2⁺ cells is 85.0 ± 1,4 % (mean ± SD, n = 3). **c**, Immunocytochemistry for PAX2 after IM induction (*day 0*). Scale bars, 50 μm. Images are representative of four independent experiments. **d**, qPCR analysis for the expression of IM markers before (*day -5*) and after IM induction (*day 0*). Genes are indicated. Data are mean ± SD (technical replicates). The experiment was repeated independently two times with similar results.

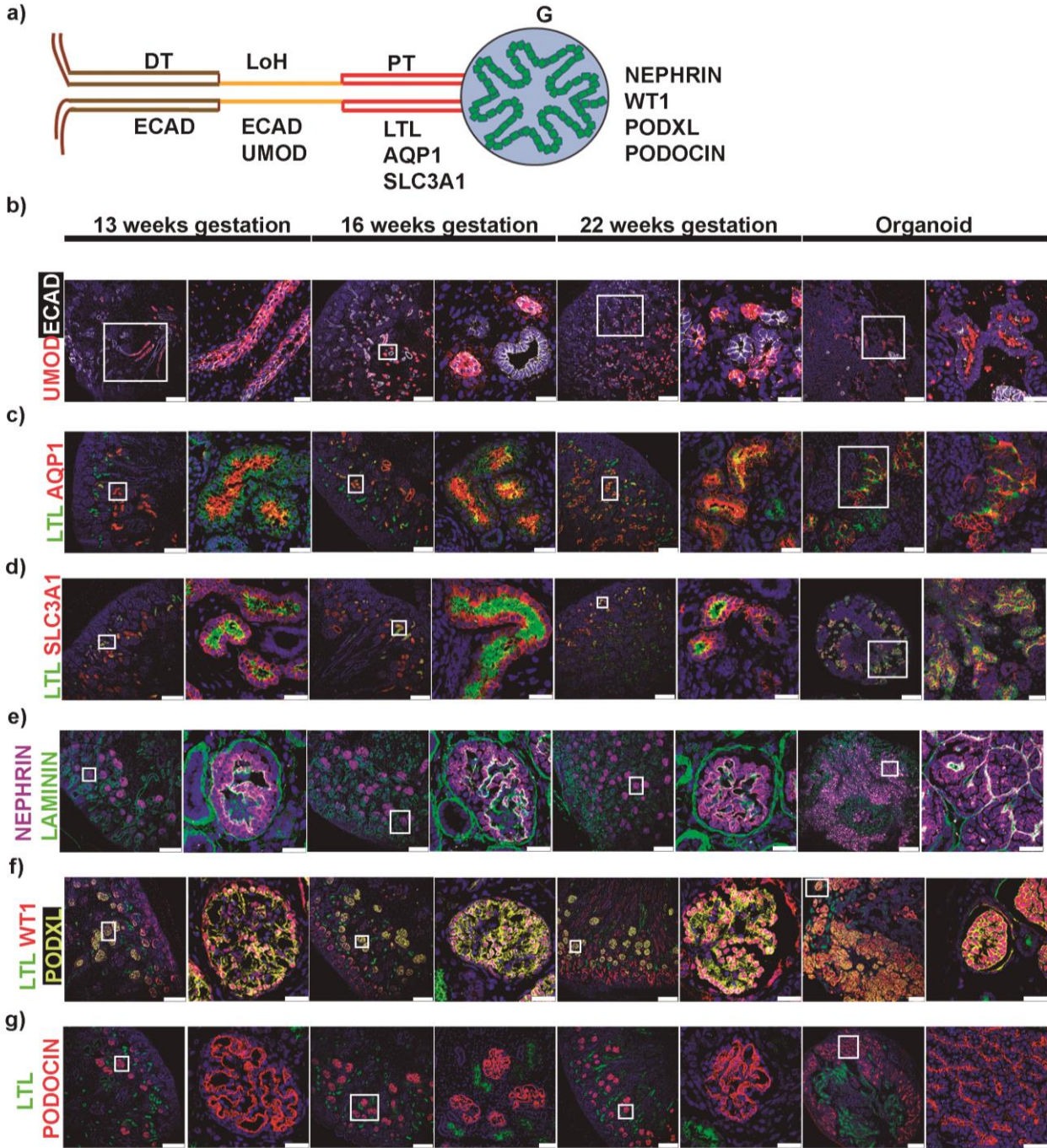
Supplementary Figure 3



Supplementary Fig. 3 | Day 8 kidney organoids express characteristic markers of RVs.

a, Bright-field and tile scan confocal images of a whole kidney organoid showing the formation of RV structures that expressed PAX2 and WT1 on *day 8* of differentiation. Scale bars, 500 μm . **b**, Hematoxylin-eosin staining of kidney organoids at *day 8*, *11*, *14* and *16* of differentiation. **c**, Schematic of the acquisition of RV proximal-distal polarity by RV-stage organoids. Markers characteristic of distal, medial and proximal identities are indicated. **d**, Immunocytochemistry for RV markers LHX1, PAX8, HNF1 β , PAX2, BRN1, ECAD and the MM marker SIX2 in *day 8* and *day 11* RV-stage organoids. Scale bars, 50 μm . Images are representative of three independent experiments (**a**, **b**, **d**). **e**, qPCR analysis for *TWIST*, *SNAI2*, *ECAD* and *WNT4* during kidney organoid differentiation (days are indicated). Data are mean \pm SD (technical replicates). The experiment was repeated independently two times with similar results.

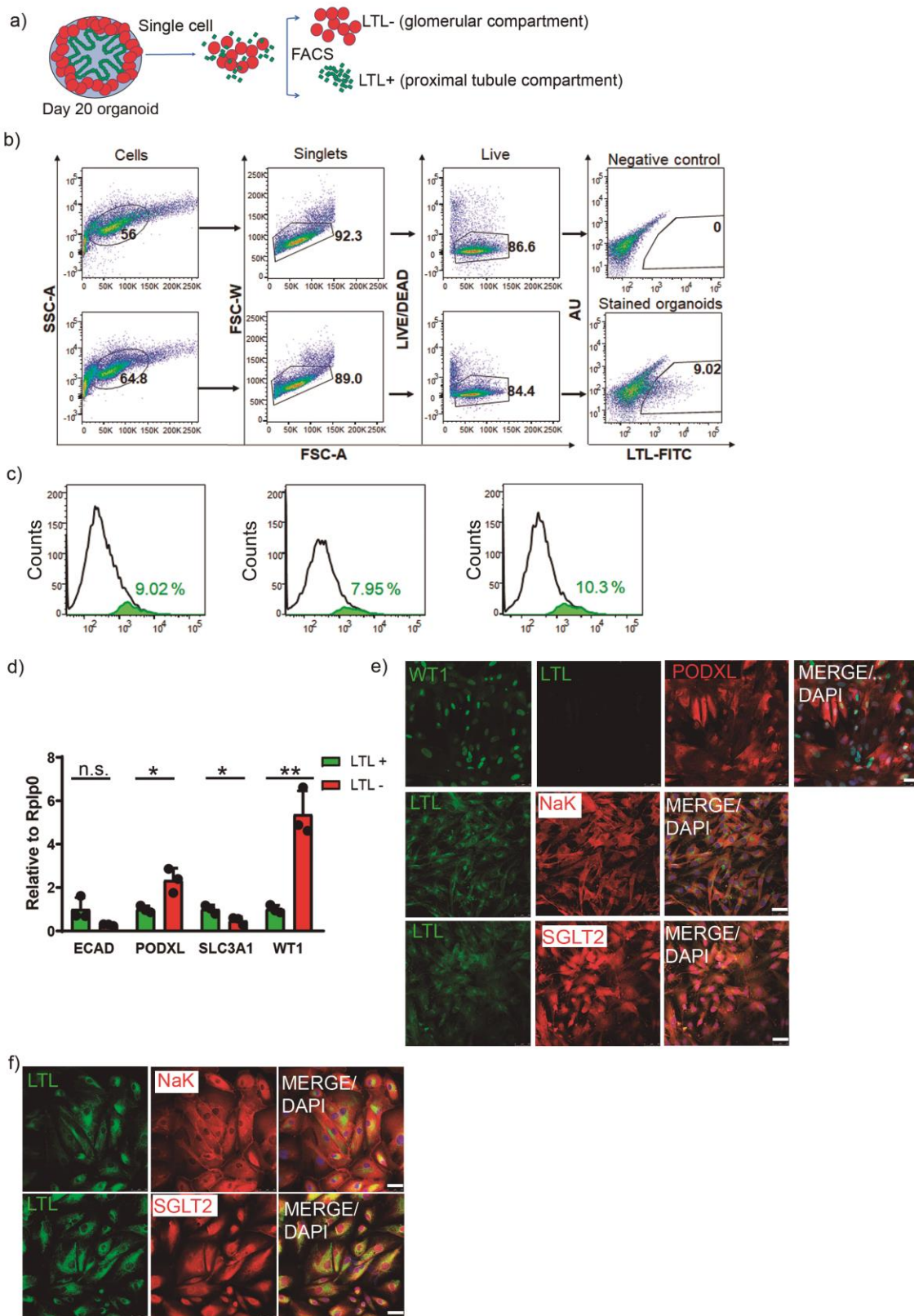
Supplementary Figure 4



Supplementary Fig. 4 | Immunohistochemistry of human fetal kidneys and kidney organoids. **a**, Schematic of a nephron illustrating the different nephron compartments, including: distal tubule (DT), Loop of Henle (LoH), proximal tubule (PT) and glomerulus (G). Characteristic late-stage nephron markers for each nephron segment are indicated. **b-g**,

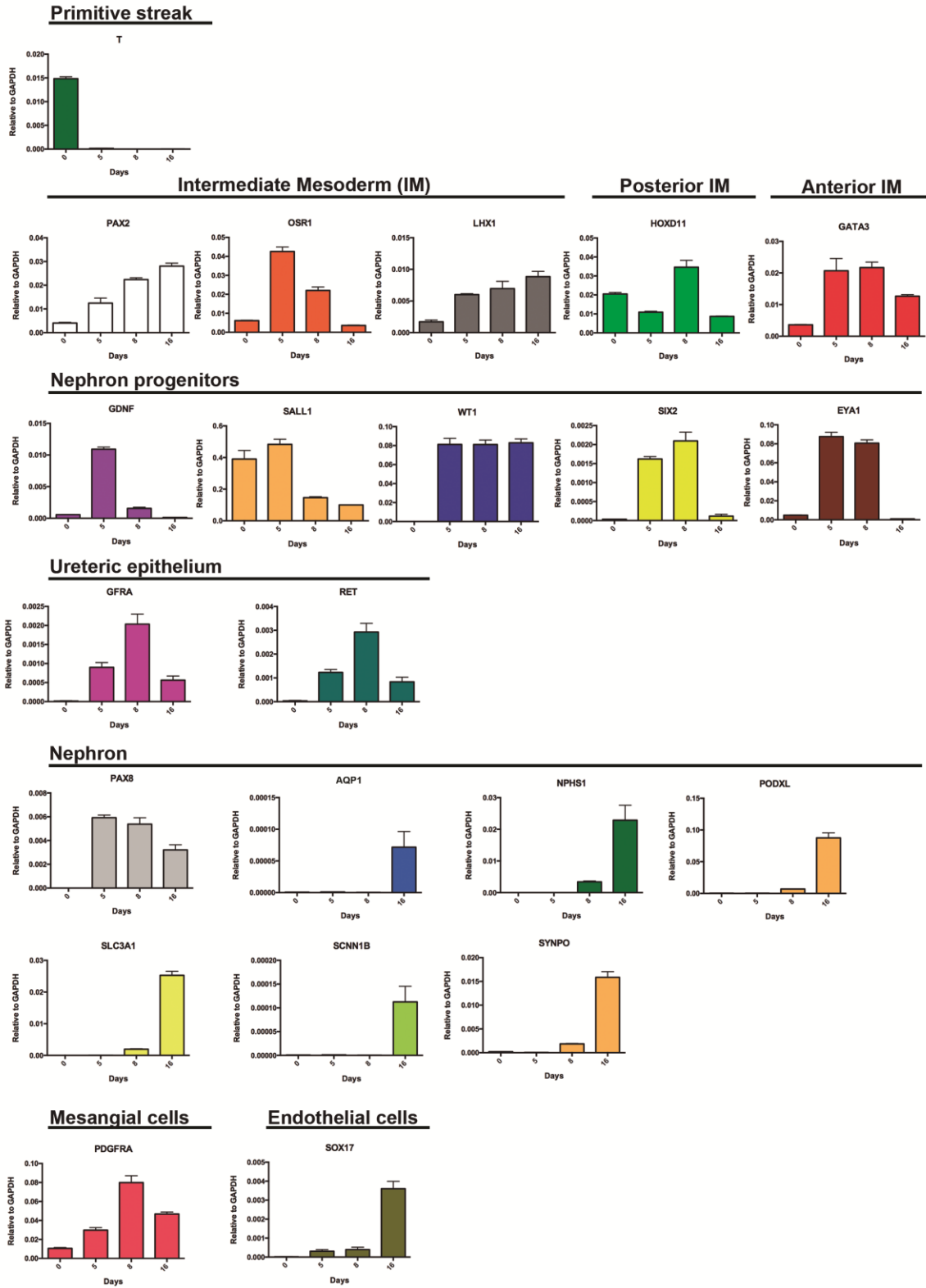
Immunohistochemistry for the indicated late-stage nephron markers in human fetal kidney samples from first (13 and 16 weeks of gestation) and second trimester (22 weeks of gestation) of gestation, and *day 16* kidney organoids. Magnified views of boxed regions are shown for all the experimental conditions. Scale bars, 250 μm and 25 μm (magnified views). One human fetal kidney sample per gestational age was analysed. Images are representative of two independent experiments.

Supplementary Figure 5



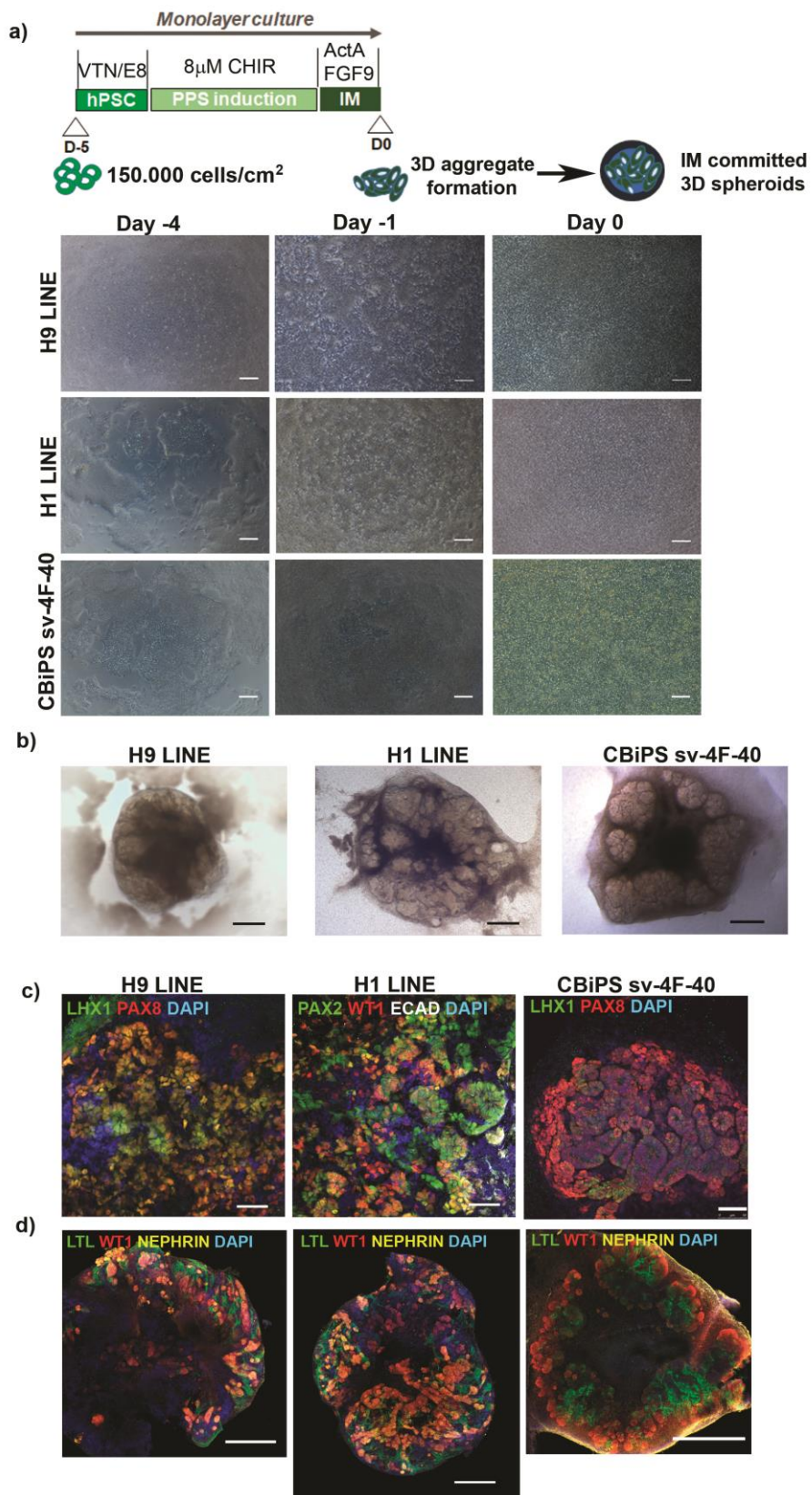
Supplementary Fig. 5 | Sorting of renal cell populations from kidney organoids. a, Schematics of the separation of glomerular (LTL^-) and tubular (LTL^+) compartments in *day 16* kidney organoids by fluorescence-activated cell sorting. Kidney organoids were stained with LTL, dissociated to single cells and sorted. **b,** Gating strategy for cell sorting of LTL^+ and LTL^- cell populations from *day 16* kidney organoids. Numbers in outlined areas indicate percent cells. AU, autofluorescence. **c,** Histograms representing the overlay of live cells and LTL^+ cells from three independent cell sorting experiments. The mean percentage of LTL^+ cells is 9.1 ± 1.2 % (mean \pm SD, $n = 3$). Each experiment is a pool of eight organoids. **d,** Total RNA was extracted from LTL^+ and LTL^- cell populations and analysed by qPCR (genes are indicated). LTL^- cells expressed higher mRNA levels for *PODXL* and *WT1* glomerular segment markers (in red) in comparison with LTL^+ cells that expressed higher mRNA levels for *ECAD* and *SLC3A1* proximal tubular markers (in green). Data are mean \pm SD. $n = 3$ independent experiments. LTL^- versus LTL^+ : *ECAD*, $t(4) = 2.3135$, ns, not significant, $P = 0.0817$; *PODXL*, $t(4) = 4.0118$, $*P = 0.016$; *SLC3A1*, $t(4) = 3.4534$, $*P = 0.026$; *WT1*, $t(4) = 6.8786$, $**P = 0.0023$. Two-tailed student's *t*-test. **e,** Immunocytochemistry for glomerulus (*WT1* and *PODXL*) and proximal tubule (*NaK*, *SGLT2*) markers in LTL^- and LTL^+ cell fractions, respectively. Images are representative of three independent experiments. **f,** Immunocytochemistry for proximal tubule markers (*NaK*, *SGLT2*) in adult human kidney proximal tubular epithelial cells that were used as positive control. One adult human kidney proximal tubular epithelial cell sample was analysed. Scale bars, 50 μ m (**e, f**).

Supplementary Figure 6



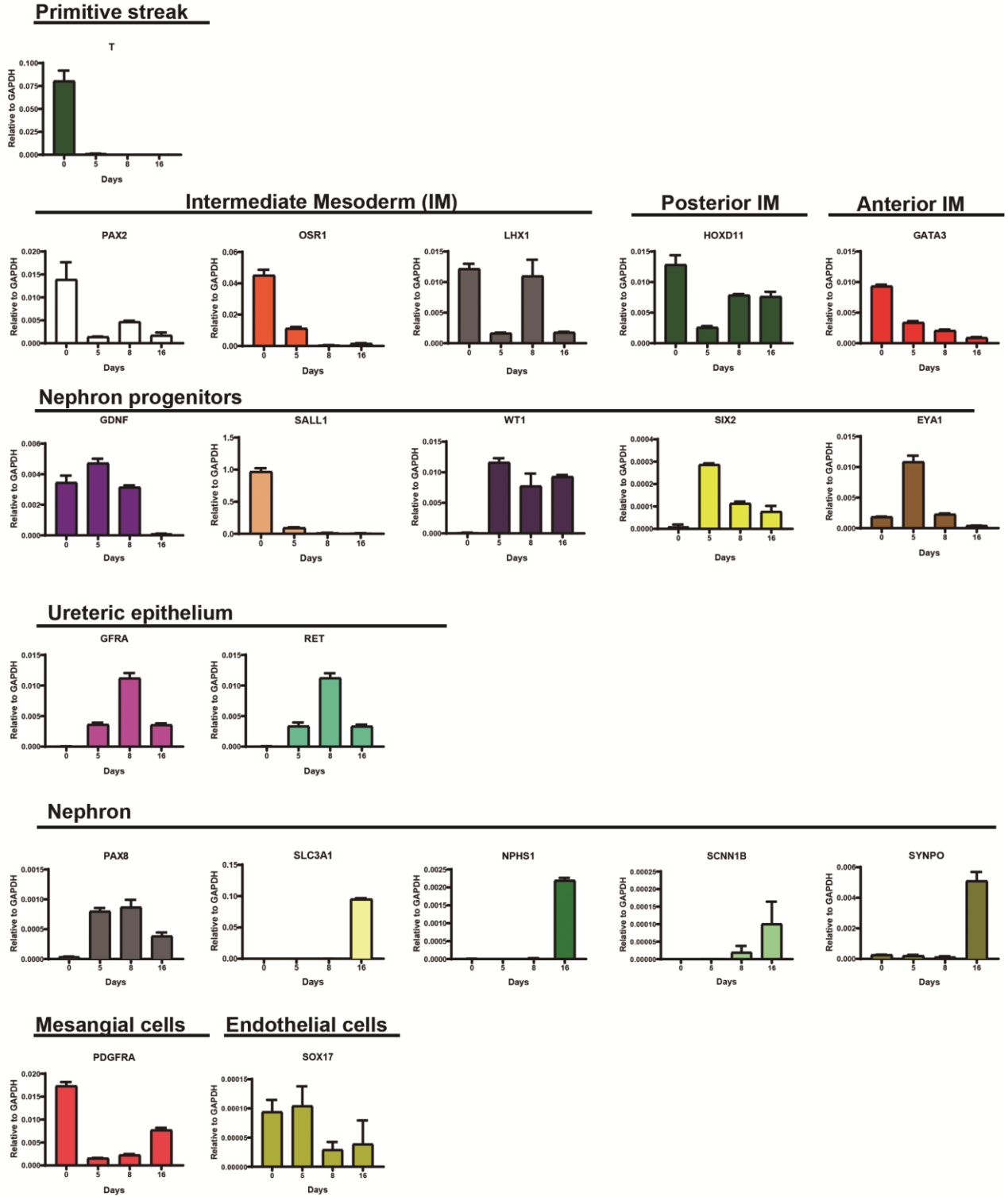
Supplementary Fig. 6 | qPCR analysis of kidney organoids from ES[4] hESC line. mRNA levels for differentiation markers were analysed by qPCR during the time course of kidney organoid differentiation at the indicated days. Markers included those for PS, IM, posterior and anterior IM, NPC, ureteric epithelium, nephron, mesangial, and endothelial cells (genes are indicated). Data are mean \pm SD (technical replicates). Each sample is a pool of six organoids per time point. The experiment was repeated independently two times with similar results.

Supplementary Figure 7



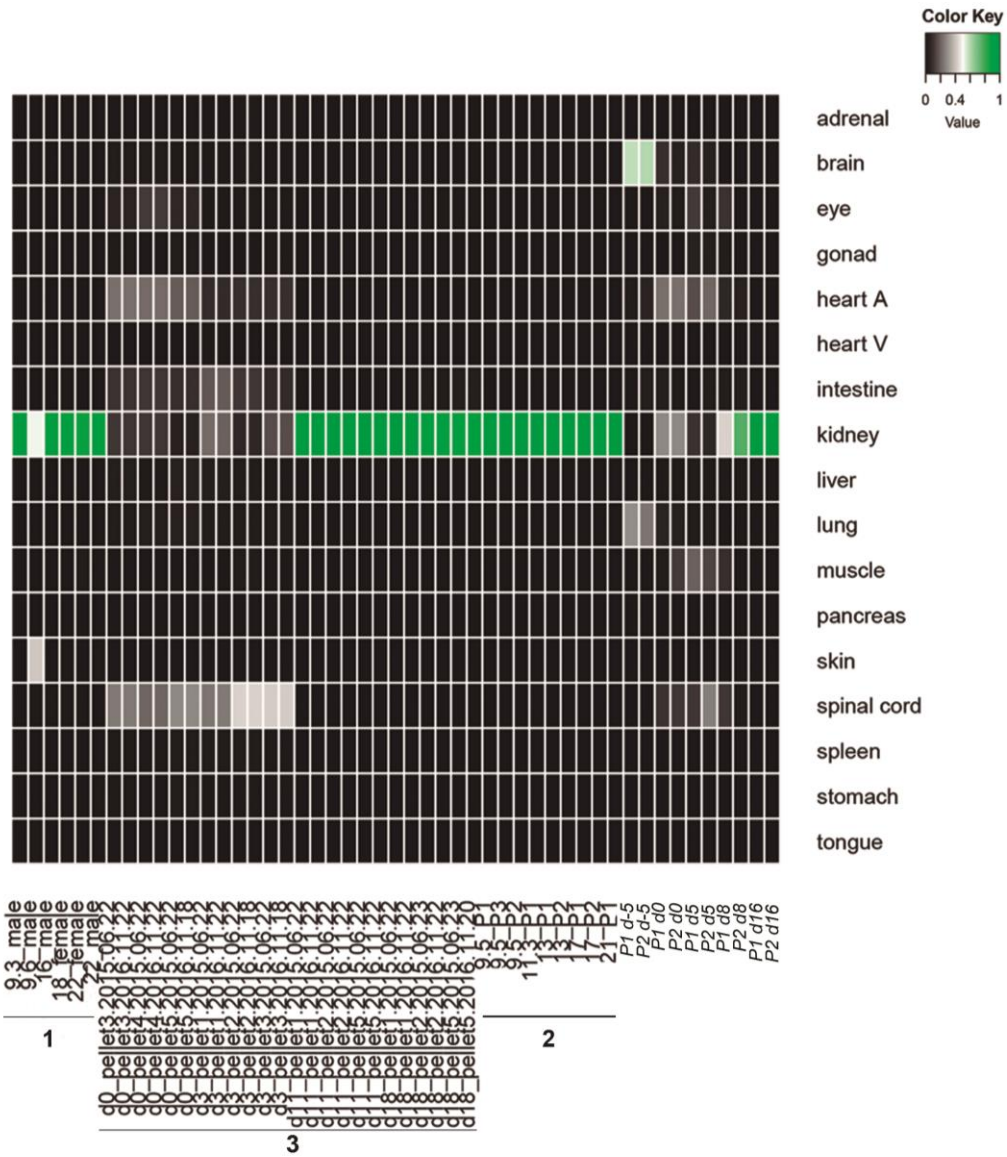
Supplementary Fig. 7 | Generation of kidney organoids from hESC and hiPSCs. a, Schematic of the timeline for the directed differentiation of hPSCs (*day -5*) into IM-committed cells (*day 0*). Culture conditions and growth factors / molecules are indicated. Bright-field images during the time course of IM induction from hESC lines (H9 and H1) and hiPSCs (CBiPS_{sv}-4F-40) (days are indicated). Scale bars, 200 μm . **b,** Bright-field images of *day 16* whole kidney organoids derived from hESC lines (H9 and H1) and hiPSCs (CBiPS_{sv}-4F-40). Scale bars, 500 μm . **c,** Immunocytochemistry for RV markers in RV-stage organoids (*day 8*) derived from the indicated hESC and hiPSC lines (markers are indicated). Scale bars, 50 μm . **d,** Immunocytochemistry for the podocyte markers NEPHRIN and WT1, and the proximal tubule marker LTL in *day 16* whole kidney organoids derived from the indicated hPSC lines. Scale bars, 500 μm . Experiments were repeated independently three times with similar results.

Supplementary Figure 8



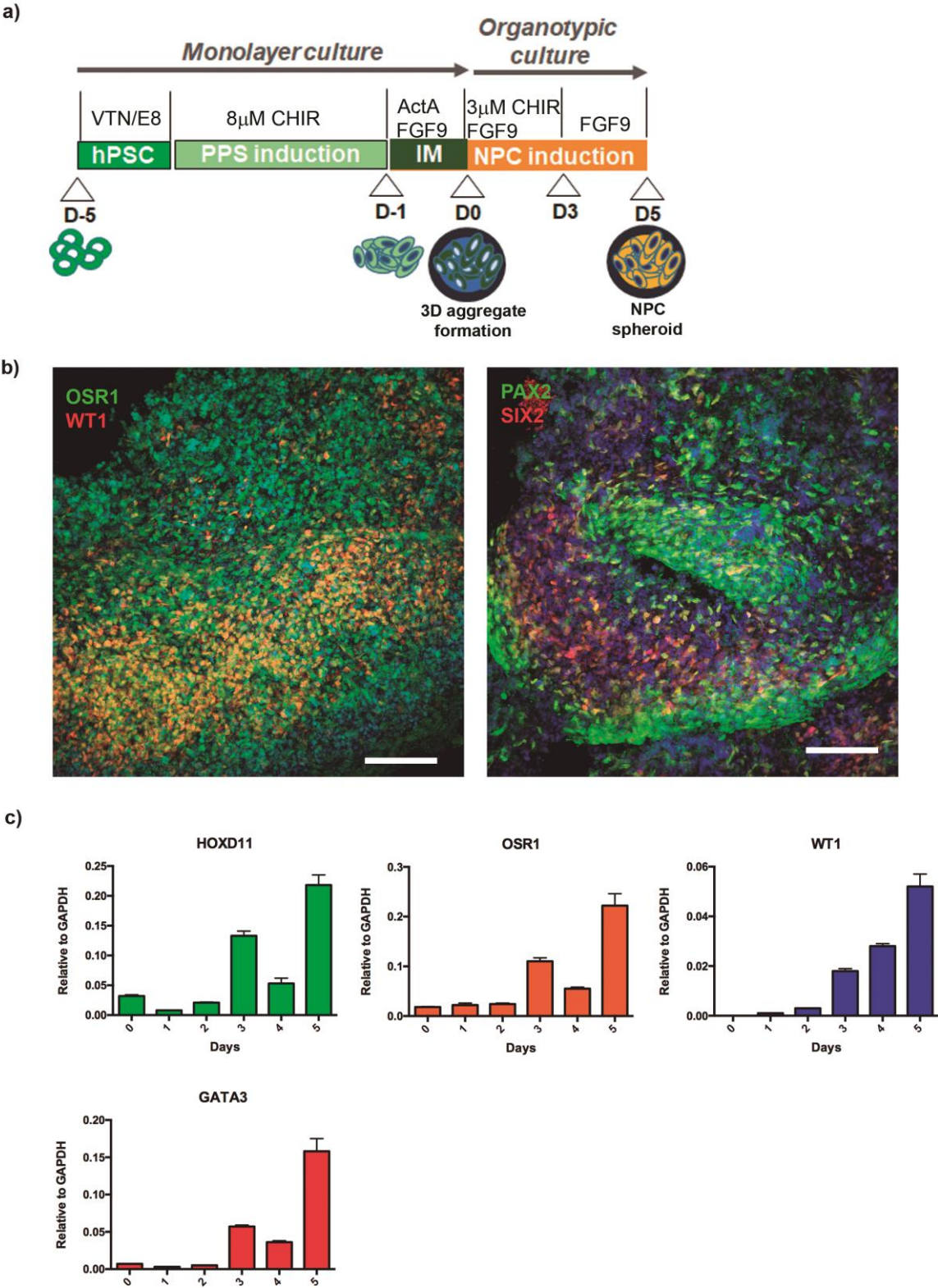
Supplementary Fig. 8 | qPCR analysis of kidney organoids from H9 hESC line. mRNA levels for differentiation markers were analysed by qPCR during the time course of kidney organoid differentiation at the indicated days. Markers included those for PS, IM, posterior and anterior IM, NPC, ureteric epithelium, nephron, mesangial, and endothelial cells (genes are indicated). Data are mean \pm SD (technical replicates). Each sample is a pool of six organoids per time point. The experiment was repeated independently two times with similar results.

Supplementary Figure 9



Supplementary Fig. 9 | Transcriptional resemblance of kidney organoids to human fetal tissues. Heat map showing the relative transcriptional identity of kidney organoids to 16 human fetal tissues. RNA-seq was performed on whole kidney organoids from 5 time points (*day -5, 0, 5, 8, and 16*) during differentiation. Six pooled organoids per time point were analysed. Two independent experiments were included in the analysis. Data from Chuva de Sousa Lopes SM [SRP055513]¹⁸ (1), McMahon AP [SRP111183]¹⁹ (2) and Little MH [SRP059518]⁹ (3) are included in the analysis.

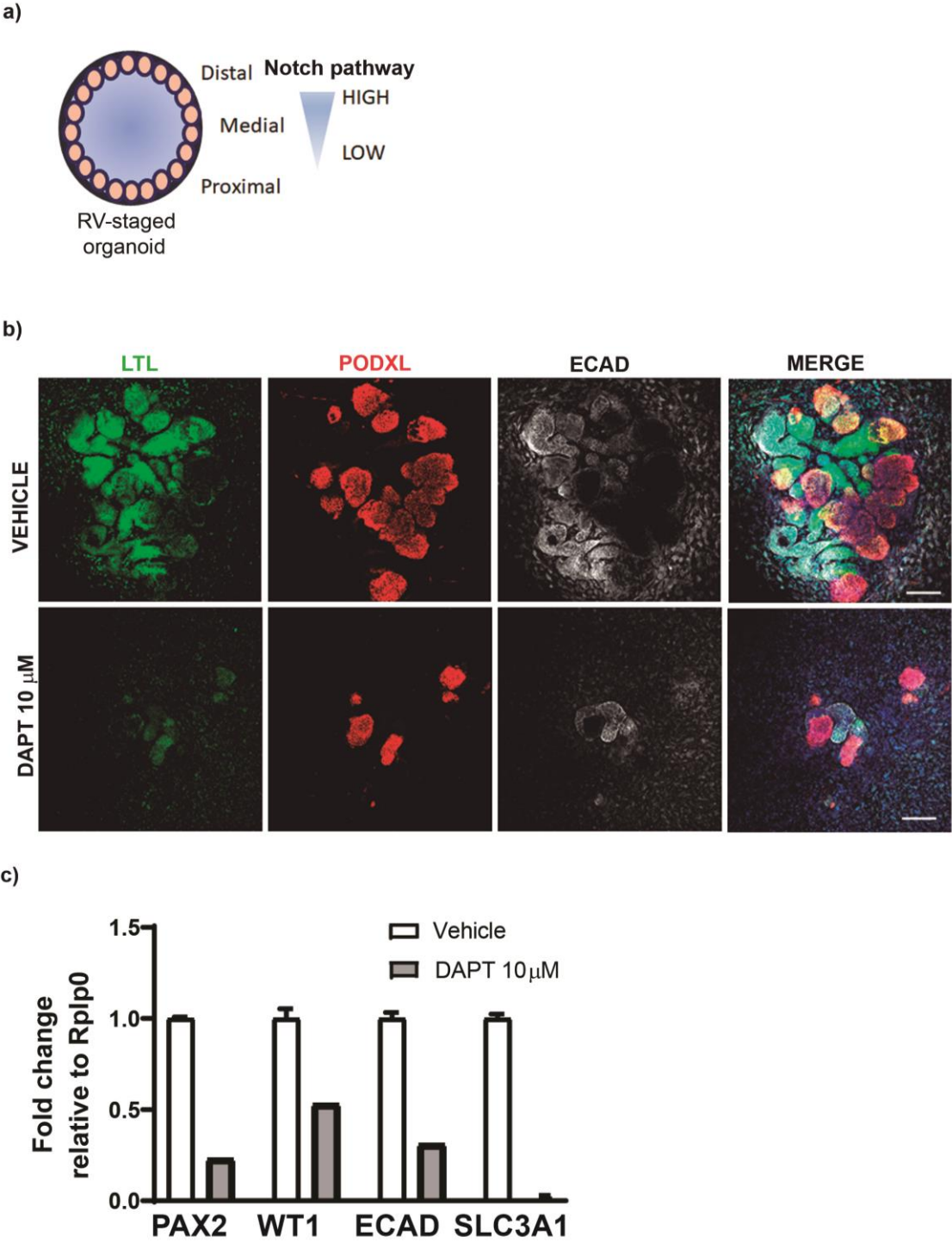
Supplementary Figure 10



Supplementary Fig. 10 | Day 5 differentiating organoids contain NPC-committed cells.

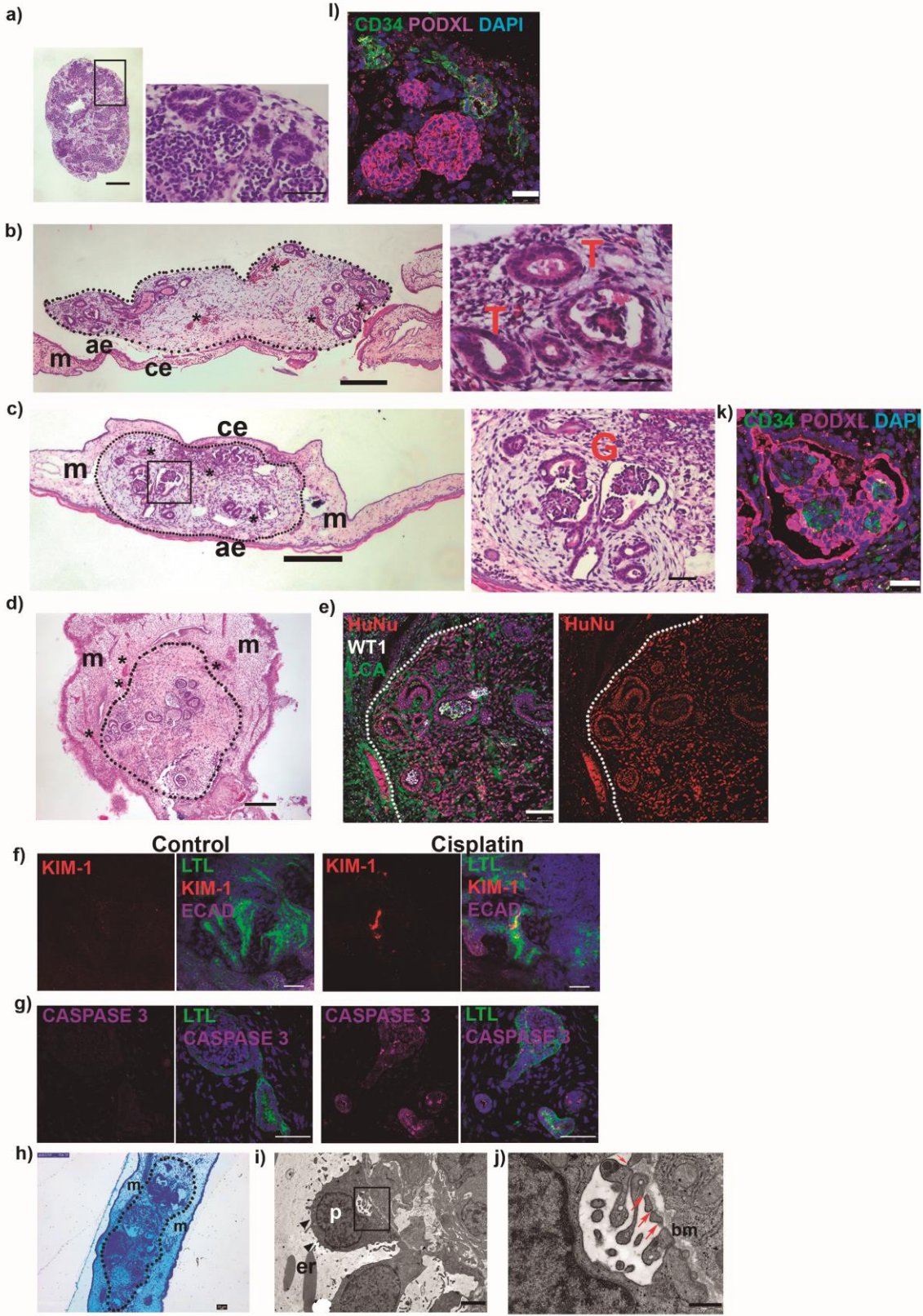
a, Schematic of the timeline for kidney organoid differentiation from the formation of IM-committed spheroids (*day 0*) to the generation of NPC-committed cells (*day 5*). Culture conditions and growth factors / molecules are indicated. **b,** Confocal images of *day 5* NPCs showing the expression of markers characteristic of the NPC signature, including OSR1, WT1, PAX2 and SIX2. Scale bars, 100 μm . **c,** qPCR analysis for *HOXD11*, *OSR1*, *WT1*, and *GATA3* during the time course of differentiation from IM to NPC-committed cells (days are indicated). Data are mean \pm SD (technical replicates). Each sample is a pool of six organoids per time point. Experiments were repeated independently two times with similar results.

Supplementary Figure 11



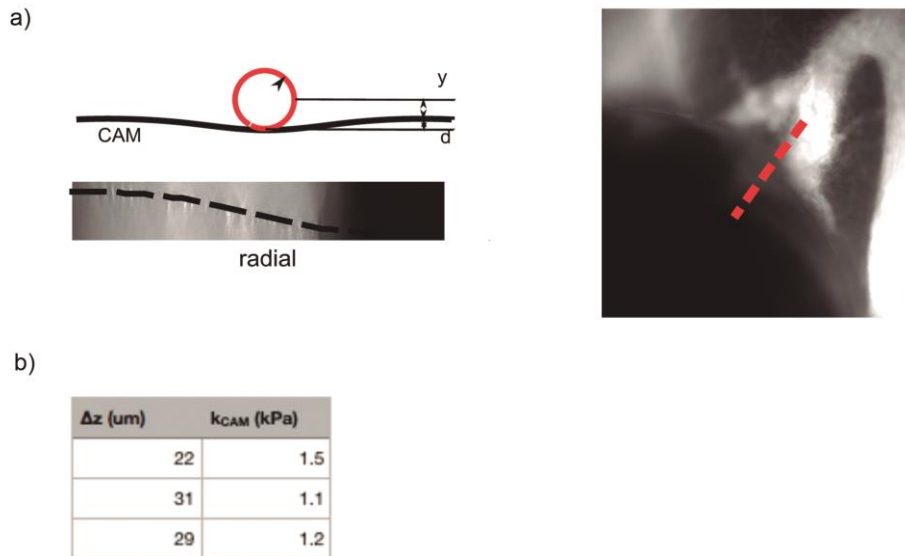
Supplementary Fig. 11 | Inhibition of Notch signaling in kidney organoids. **a**, Model of predicted alterations in nephron patterning when inhibiting Notch signaling with the γ -secretase inhibitor (DAPT) in kidney organoids from *day 8* to *day 16* of differentiation. **b**, Immunocytochemistry for proximal tubule-like structures (LTL, ECAD) and podocyte-like cells (PODXL) in kidney organoids treated with vehicle, or DAPT (10 μ M) for 8 days. Scale bars, 50 μ m. **c**, qPCR analysis of *day 16* kidney organoids treated with vehicle, or DAPT (10 μ M) for 8 days (genes are indicated). Data are mean \pm SD (technical replicates). Each sample is a pool of four organoids per time point. Experiments were repeated independently three times with similar results.

Supplementary Figure 12



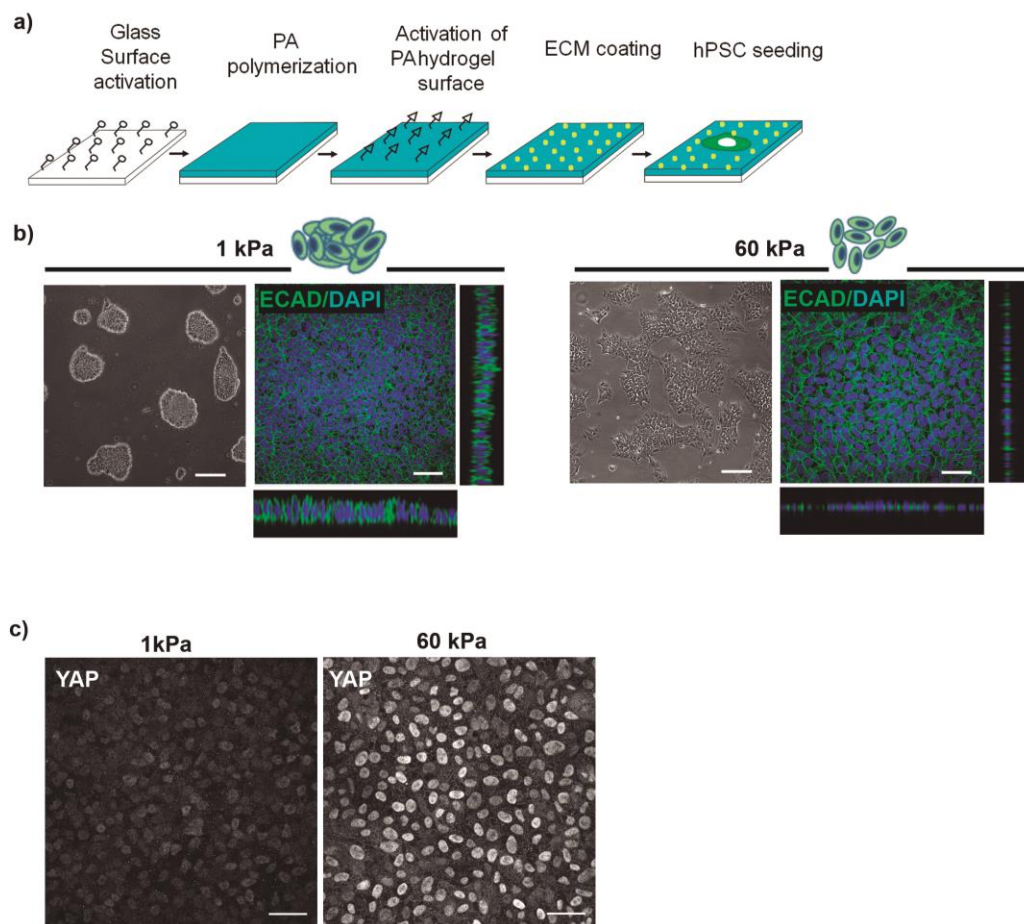
Supplementary Fig. 12 | Implantation of kidney organoids into the chick CAM. a-d, Hematoxylin-eosin staining of *in vitro* maintained (**a**) and implanted kidney organoids (**b-d**). Chorionic epithelium (ce). Allantoic epithelium (ae). Mesenchyme (m). Blood vessels (asterisks). Tubule-like (T) and glomeruli-like (G) structures. The estimated organoid dimension (area of a middle organoid section) is 0.93 (**a**), 0.66 (**b**), 0.29 (**c**), 0.98 (**d**) mm². Scale bars, 250 μ m and 50 μ m (magnified views). Images are representative of n = 5 biologically independent *in vitro* maintained (**a**) and n = 8 biologically independent implanted organoids (**b-d**) from three independent experiments. **e**, Immunohistochemistry of **d** for LCA, HuNu and WT1. Scale bars, 75 μ m. Images are representative of n = 2 biologically independent implanted organoids from two independent experiments. **f, g**, Immunohistochemistry for LTL, KIM-1, ECAD (**f**) and cleaved Caspase 3, LTL (**g**) in implanted kidney organoids (control: injected with saline) and 24 h after cisplatin injection. Scale bars, 50 μ m. The experiment was performed independently two times with similar results. **h**, Semithin section of an implanted kidney organoid (dashed line). Scale bar, 200 μ m. **i, j**, TEM of implanted kidney organoids. **i**, Podocyte-like cells (p) exhibiting apical microvilli (indicated with black triangles), and primary and secondary processes. Basement membrane (bm). Chicken erythrocytes (er). **j**, A magnified view of **i** showing primitive slit diaphragm-like structures (red arrows) between the cell processes. Scale bars, 2 μ m (**i**) and 500 nm (**j**). Images (**h-j**) are representative of n = 2 biologically independent implanted organoids from two independent experiments. **k, l**, Immunohistochemistry for CD34 and PODXL in implanted (**k**) and *in vitro* maintained (**l**) kidney organoids. Scale bars, 25 μ m. Images are representative of n = 2 biologically independent implanted organoids from two independent experiments (**k**), and n = 3 biologically independent *in vitro* maintained organoids from three independent experiments (**l**).

Supplementary Figure 13



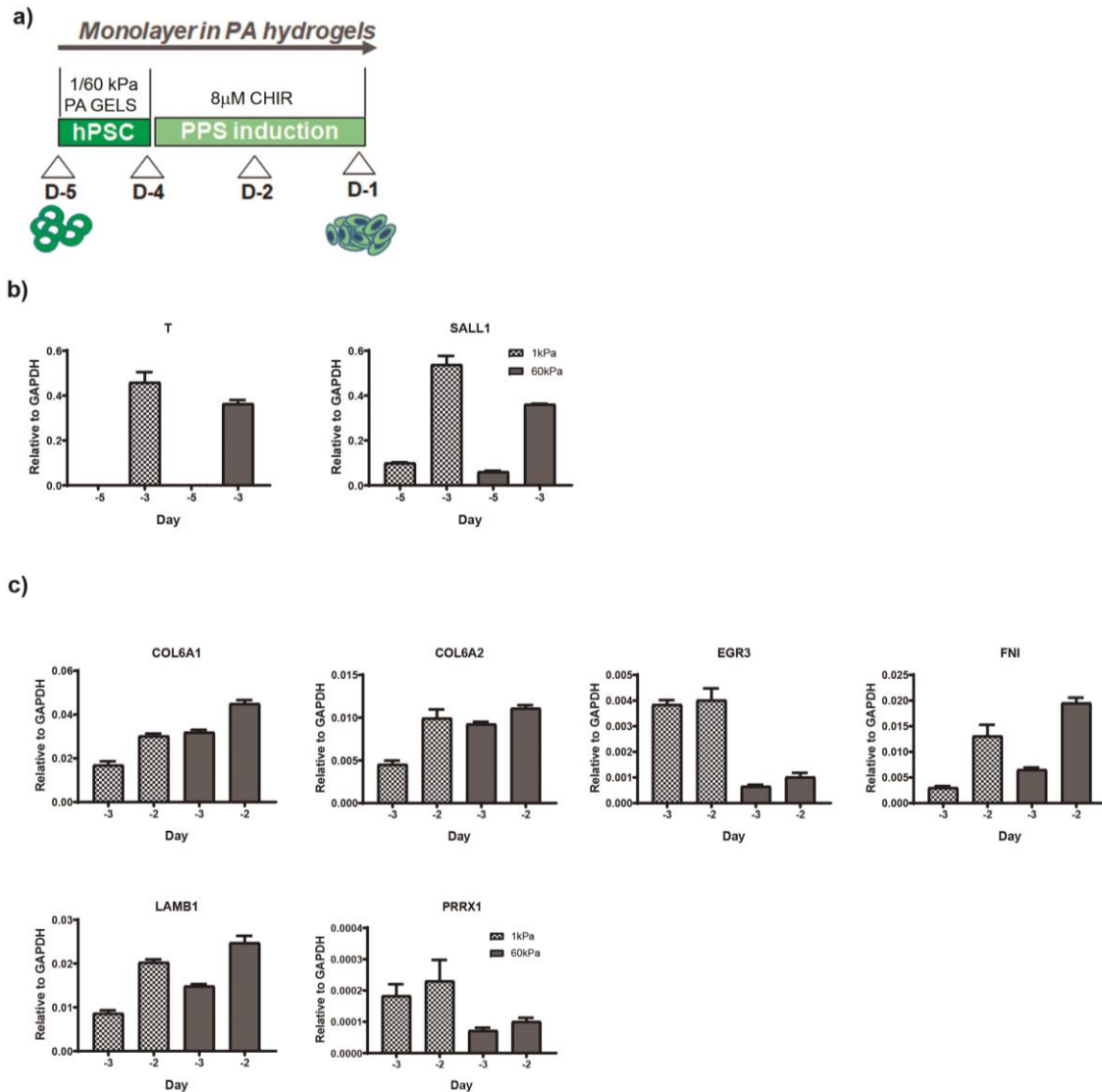
Supplementary Fig. 13 | Measurement of the chick CAM stiffness. **a**, Schematic of the ball indentation method (left panel). Using a custom made Matlab code, the indentation depth (d) was determined based on the derivative of the fluorescence intensity profile of the FITC-labeled CAM along a line crossing the border of the ball (red dashed line in right panel). **b**, Young modulus values of the chick CAM measured using the ball indentation method from three separate experiments.

Supplementary Figure 14



Supplementary Fig. 14 | Fabrication of hydrogels with controlled stiffness. **a**, Schematic of the methodology for the fabrication of functionalized polyacrylamide (PA) hydrogels for the directed differentiation of hPSCs. Glass surface is activated prior polymerization of the PA hydrogel (light blue) on top of the activated glass. After surface activation NHS ester groups are available to bond to free amines of the ECM proteins (yellow dots) and then hPSCs (green) are allowed to adhere under undifferentiated culture conditions. **b**, Bright-field and confocal images for ECAD expression in hPSCs grown on soft (1 kPa) and rigid (60 kPa) PA hydrogels under undifferentiated culture conditions. Scale bars, 100 μm (bright field images) and 50 μm (confocal images). **c**, Confocal images for YAP immunofluorescence in hPSCs grown on soft (1 kPa) and rigid (60 kPa) PA hydrogels under undifferentiated culture conditions. Scale bars 50 μm . Experiments were repeated independently three times with similar results.

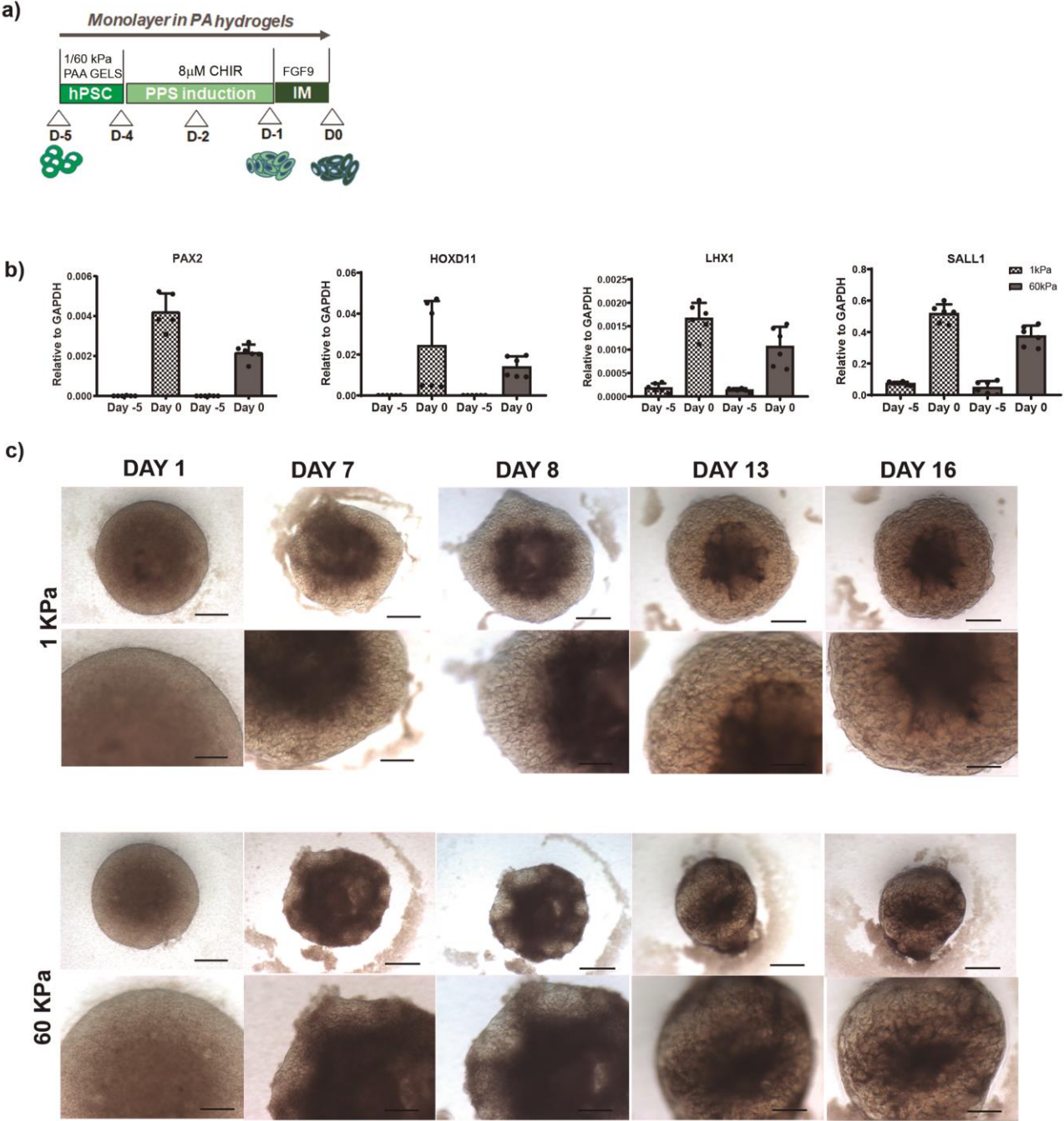
Supplementary Figure 15



Supplementary Fig. 15 | Induction of PPS-committed cells in soft and rigid substrates.

a, Schematic of the timeline for the directed differentiation of hPSCs (*day -5*) into PPS-committed cells (*day -1*) under 2D monolayer culture conditions. **b**, mRNA levels for the indicated genes analysed by qPCR at *day -5* and *day -3* of the PPS induction under soft (1 kPa) and rigid (60 kPa) conditions. **c**, mRNA levels for the indicated genes analysed by qPCR at *day -3* and *day -2* of PPS induction under soft (1 kPa) and rigid (60 kPa) conditions. Data are mean \pm SD (technical replicates). Experiments were repeated independently two times with similar results.

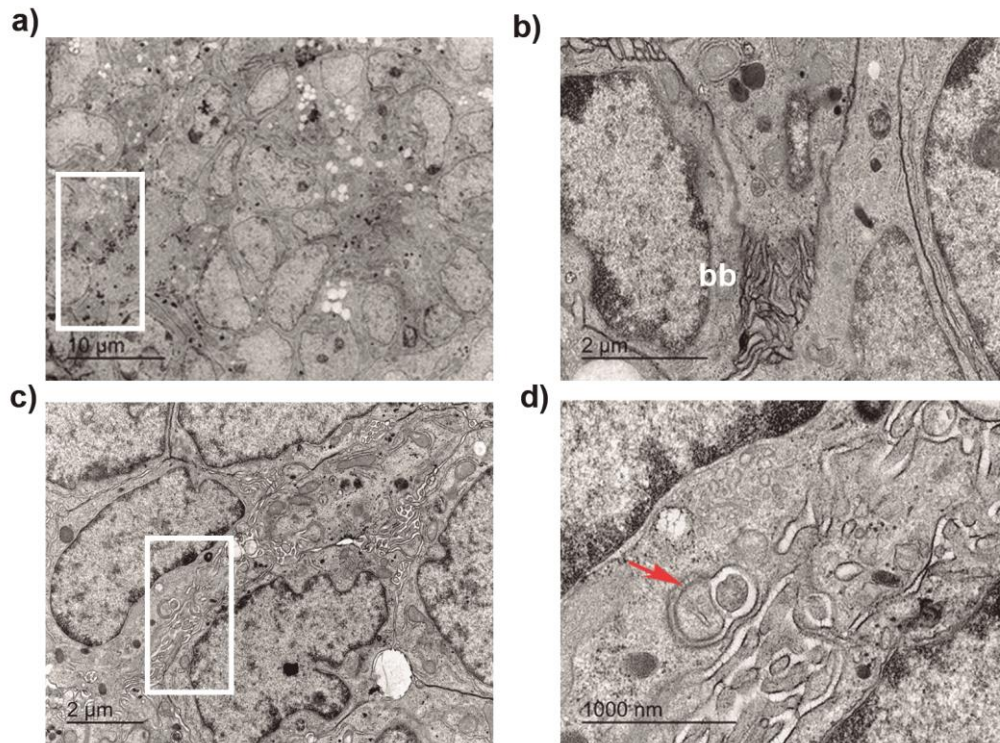
Supplementary Figure 16



Supplementary Fig. 16 | Induction of IM-committed cells in soft and rigid substrates.

a, Schematic of the timeline for the directed differentiation of hPSCs (*day -5*) into IM-committed cells (*day 0*) in soft (1 kPa) and rigid (60 kPa) PA hydrogels. **b**, mRNA levels for the indicated genes analysed by qPCR at *day -5* and *day 0* of IM induction under soft (1 kPa) and rigid (60 kPa) conditions. Data are mean \pm SD, n = 2 independent experiments. Three technical replicates are shown per sample. **c**, Bright field images of kidney organoids derived in soft (1 kPa) or rigid (60 kPa) conditions during differentiation (days are indicated). Scale bars, 500 μ m and 250 μ m (magnified views). Images are representative of n = 10 kidney organoids (1 kPa) and n = 10 kidney organoids (60 kPa) from three independent experiments.

Supplementary Figure 17



Supplementary Fig. 17 | TEM of kidney organoids from 60 kPa PA hydrogels. a-d, TEM of *day 16* kidney organoids generated using 60 kPa PA hydrogels. **a**, Tubular-like structures with epithelial cells that exhibit high mitochondrial content and brush borders. **b**, A magnified view of the boxed region in **a** showing a detail of brush borders (bb). **c**, Differentiated podocyte-like cells exhibiting cell processes. **d**, A magnified view of the boxed region in **c** showing immature slit diaphragm-like structures (indicated with a red arrow). Scale bars, 10 µm (**a**), 2 µm (**b**), 2 µm (**c**) and 1000 nm (**d**). Images are representative of two independent experiments.

Supplementary Tables

Supplementary Table 1. RNA-seq values across samples at the indicated time frames for Keygenes analysis.

Supplementary Table 2. Normalized RNA-seq values across samples at the indicated time frames for clustering analysis after correction for batches effect.

Supplementary Table 3. Genes found to be significantly down or up-regulated in hESCs grown for 24 h (*day -4*) on soft (1 kPa) compared to rigid (60 kPa) PA hydrogels. Difference in expression is reported as log fold change (see Methods). $n = 4$. Adjusted P value smaller than 0.05 (Wald Test).

Supplementary Table 4. Genes found to be significantly down or up-regulated in hESCs differentiated on soft (1 kPa) compared to rigid (60 kPa) PA hydrogels at *day -3* and *day -2* of the differentiation process. Difference in expression is reported as log fold change (see Methods). Genes are grouped according to their biological function. $n = 4$. Adjusted P value smaller than 0.05 (Wald test).

Supplementary Table 5. List of primary antibodies used in immunocytochemistry and immunohistochemistry.

Supplementary Table 6. List of primers used for RT-qPCR analysis.

Gene	Forward	Reverse
<i>CDX1</i>	CGTTACATCACAAATCCGGCG	CCAGATCTTCACCTGCCGTT
<i>CDX2</i>	GAACCTGTGCGAGTGGATG	GGATGGTGTAGTAGCGACTG
<i>CER1</i>	GTGCCCTTCAGCCAGACTA	CAGACCCGCATTTCCCAA
<i>CRIPTO</i>	CGGAAGTGTGAGCACGATGT	GGCAGCCAGGTGTCATG
<i>ECAD</i>	CGAGAGCTACACGTTACGG	GGGTGTCGAGGGAAAAATAGG
<i>EOMES</i>	TGCAGGGCAACAAAATGTATG	GTCTCATCCAGTGGGAACAGTA
<i>EVX1</i>	GAAGAAAATCGAGGGTCCGGC	CCGTTGCTCTGGGGGTC
<i>EYA1</i>	ATCTAACCAGCCCGCATAGC	GTGCCATTGGGAGTCATGGA
<i>ENDOGLIN</i>	CCTACGTGTCTCTGGCTCATC	GGTGTGTCTGGGAGCTTGAA
<i>FGF4</i>	GGTGAGCATCTTCGGCGT	CTCATCGGTGAAGAAGGGCG
<i>FOXA2</i>	GTGAAGATGGAAGGGCACG	CATGTTGCTCACGGAGGATAG
<i>GAPDH</i>	AGCAATGCCTCCTGCACCACCAAC	CCGGAGGGGCCATCCACAGTCT
<i>GATA3</i>	CGTCTGTGCGAACTGTCA	GTCCCCATTGGCATTCTCC
<i>GDNF</i>	CCAACCCAGAGAATTCAGA	AGCCGCTGCAGTACCTAAAA
<i>GFRα1</i>	AAGCACAGTACGGAATGCT	GTTGGGCTTCTCCCTCTCTT
<i>GSC2</i>	CCAGTATCCTGACGTGAGTACG	GGTCTTGAACCAGACCTCCA
<i>HOXD11</i>	GCCAGTGTGCTGTCGTTCCC	CTTCCTACAGACCCCGCCGT
<i>LHX1</i>	CTTCTTCCGGTGTTCGGTA	TCATGCAGGTGAAGCAGTTC
<i>MIXL1</i>	GGTACCCCGACATCCACTTG	ACCTGGAAGAGGGGAGAAAA
<i>NANOG</i>	CAAAGGCAAACAACCCACTT	TCTGCTGGAGGCTGAGGTAT
<i>NODAL</i>	TGTTGGGGAGGAGTTTCATC	GCACAACAAGTGAAGGGAC
<i>NPHS1</i>	GGCTCCCAGCAGAAACTCTT	CACAGACCAGCAACTGCCTA
<i>OCT4</i>	AGTGAGAGGCAACCTGGAGA	ACACTCGGACCACATCCTTC
<i>OSR1</i>	CTGCCAACCTGTATGGTTT	CGGCACTTTGGAGAAAGAAG
<i>PAX2</i>	CCCAAAGTGGTGGACAAGAT	GAAAGGCTGCTGAACTTTGG
<i>PAX8</i>	GGCTCCACCTCATCCATCAA	CTGCTGCTGCTCTGTGAGTC
<i>PDGFRA</i>	GAGCGCTGACAGTGGCTACAT	TCGTCCTCTCTTGTATGAAGGT
<i>PODXL</i>	GATAAGTGCGGCATAACGGCT	GCTCGTACACATCCTTGCCA
<i>RET</i>	CTCGACGACATTTGCAAGAA	AGCATTCCGTAGCTGTGCTT
<i>RPLP0</i>	CCATTCTATCATCAACGGGTACAA	AGCAAAGTGGGAAGGTGTAATCC
<i>SALL1</i>	TCATGTCCGAGCAGTTCAAG	TCCCAGTGTGTGCTCTGTA
<i>SCNN1B</i>	CCTGGAAGTGAATTCGGCCT	GGGTATGACCTCTGCTCGTG
<i>SIX2</i>	GGCCAAGGAAAGGGAGAACA	GAGCTGCCTAACACCGACTT
<i>SLC3A1</i>	CACCAATGCAGTGGGACAAT	CTGGGCTGAGTCTTTTGAC
<i>SMAD2</i>	CCAGAAACGCCACCTCCTG	GCTGGAGAGCCTGTGTCCA
<i>SNAI2</i>	CGAACTGGACACACATACAGTG	CTGAGGATCTCTGGTTGTGGT
<i>SOX17</i>	AGCAGAATCCAGACCTGCAC	TTGTAGTTGGGGTGGTCTCTG
<i>SYNPO</i>	GCTGAGGAGGTGAGATGCAG	CTCTGGAGAAGGTGCTGGTG
<i>T</i>	GCAAAAAGCTTTCTTGATGC	ATGAGGATTTGCAGGTGGAC
<i>TBX6</i>	CATCCACGAGAATTGTACCCG	AGCAATCCAGTTTAGGGGTGT
<i>TWIST1</i>	GTCCGCAGTCTTACGAGGAG	GCTTGAGGGTCTGAATCTTGCT
<i>VEGFR</i>	CACATTGGCCACCATCTGAAC	CCATCAGAGGCCCTCCTTG
<i>WNT4</i>	TCGTCTTCGCCGTCTTCTCAG	GGCCCTTGAGTTTCTCGCAC
<i>WT1</i>	GCGGAGCCCAATACAGAATA	GATGCCGACCGTACAAGAGT

Supplementary Table 7. Summary of statistics and reproducibility information.

Supplementary Video Files

Supplementary video 1. Evidence for the circulation of chick blood within an implanted kidney organoid at day 3 of the implantation period. Video recording was performed in n = 3 biologically independent implanted kidney organoids with similar results.

Supplementary video 2. Evidence for the circulation of chick blood within an implanted kidney organoid at day 5 of the implantation period. White arrow indicates a blood vessel going through the kidney organoid. Video recording was performed in n = 2 biologically independent implanted kidney organoids with similar results.

Supplementary video 3. Evidence for the circulation of chick blood within an implanted kidney organoid at day 5 of the implantation period after intravital injection of dextran-FITC into the CAM vasculature. Intravital injection of dextran-FITC was performed in n = 3 biologically independent implanted kidney organoids with similar results.